Failed Rib Regions in a Computational Human Model vs. Observed PMHS Fractures: A Comparative Study

Berkan Guleyupoglu[1,2], Ryan Barnard[1], F. Scott Gayzik[1,2]
[1]Wake Forest University School of Medicine [2]Virginia Tech – Wake Forest Center for Injury Biomechanics

ABSTRACT

The objective of this study is to compare failed regions (FRs) in the ribs from a computational human body model using two different methods vs. PMHS rib fractures observed in published biomechanics tests. The Global Human Body Models Consortium 50th percentile male occupant model was used in all simulations. Fourteen simulations were conducted with rib FRs either predicted probabilistically (PFR) or deterministically (DFR). The impacts were as follows: a 6.7 m/s chest hub, a 12.0 m/s lateral plate, a 6.7 m/s shoulder hub, a 6.7 m/s thoracoabdominal hub, a 6.0 m/s abdominal bar, a 10 m/s lateral pelvis, and a 6.7 m/s Heidelberg-type lateral sled. Prediction of DFRs was achieved through a scheme that analyzes eliminated elements based on effective plastic strain exceeding 0.018 in 4 contiguous elements. Prediction of PFRs used an analysis of maximum principle strains in the ribs and a default age of 35 years. In the pelvic block impact there was 1 DFR and 2 PFRs compared with an average of 1.5 fractures found by Bouquet et al, 1998. The lateral plate impact had higher predictions with 43 DFRs and 28 PFRs whereas the average fracture count in the study by Kemper et al, 2008 was 22.5. The chest hub impact conducted by Kroell et al (1971, 1974) found 9.4 ± 7.2 fractures and in our simulations, 5 DFRs and 11 PFRs were predicted. Finally, in the lateral sled case, 21 PFRs and 26 DFR's were predicted compared to an average of 14 in the PMHS tests. The average age of all PMHS was 64.8 years old. The criteria for FRs should to be further tuned to match experimental values. When fracture counts are high in the experiments, the DFRs and PFRs surprisingly both exceed the reported value, despite the lack of eliminated elements in the PFR scheme. However, in cases where fractures were low, better agreement was found between experimental, DFR and PFR predictions. Future work will focus on the effect of cortical thickness, and age as a predictor; either making material adjustments as function of age in the DFR scheme or explicitly accounting for it in the PFR scheme.

INTRODUCTION

The most common skeletal injury that a restrained occupant will sustain during a frontal collision are rib fractures (Pattimore, et al., 1992). Anthropomorphic test devices (ATDs) commonly used to determine injury risk based on correlative predictions of thoracic injury for consumer and regulatory tests, however are currently unable to determine localized injury (e.g. rib fracture). PMHS can be instrumented to measure local rib strains however have a high overhead cost and the use of which is complicated through specimen variability in relevant

measures (eg. age, bone mineral density, etc.). Computational human body models are another potential tool that can be used for the study of localized injury.

The Global Human Body Models Consortium (GHBMC) 50th percentile male model (M50) was utilized in this study. The human body finite element model CAD data was obtained through multi-modality imaging (Gayzik, et al., 2011). A consortium of universities developed and validated models of the head (Mao, et al., 2013; Takhounts, et al., 2013; Yanaoka, et al., 2013), neck (Barker, et al., 2017; DeWit, et al., 2012; Fice, et al., 2011; Mattucci, et al., 2013; Mattucci, et al., 2012), thorax (Li, et al., 2010a; Li, et al., 2010b; Poulard, et al., 2015), abdomen (Soni, et al., 2013), pelvis (Kim, et al., 2012), and lower extremity (Shin, et al., 2013; Untaroiu, et al., 2013; Yue, et al., 2011; Yue, et al., 2014). Once regionally validated, the models were integrated into a full body model and validated in hub impacts and sled tests (Decker, et al., 2017; GHBMC, 2014; Hayes, et al., 2014; Park, et al., 2013; Vavalle, et al., 2014; Vavalle, et al., 2013a; Vavalle, et al., 2013b; Vavalle, et al., 2013c).

Failure in the rib cage of the GHBMC M50 model can be included through element erosion. For an element to be eroded and thereby removed from calculation, the effective plastic strain needs to reach a user-defined limit. Effective plastic strain calculations only occur once a user-defined yield stress condition is surpassed. In the yield regime, effective plastic strains are increased and remain at their level if stress is reduced. However other methods exist to predict failure, such as a probabilistic framework introduced by Forman et al (Forman, et al., 2012). In this framework, failure is determined through post-processing of principal strains and yields a risk of failure. The model is solved with element erosion disabled in these scheme.

Previous studies in literature have investigated, through visual inspection, the amount of failures that have occurred in GHBMC models and found reasonable agreement with experimental fractures (Davis, et al., 2016; Hayes, et al., 2014; Schoell, et al., 2015; Vavalle, et al., 2015; Vavalle, et al., 2013b). However, visual inspection of the rib cage of the model does not allow for a quick and repeatable method by which to determine failure in the model. We sought to validate an automated probabilistic and deterministic approach of evaluating failures in the rib cage against PMHS fracture data in this study.

The objective of this study is to use the GHBMC detailed human body occupant model (M50-O; v. 4.4) to study the differences in prediction between deterministic and probabilistic methods of rib injury prediction and experimental results. Furthermore, investigate the differences in failure predictions between the two methods themselves.

METHODS

The Global Human Body Models Consortium (GHBMC) 50th percentile male occupant model (M50-O, v4.4) was used in all simulations. Fourteen simulations were conducted with rib FRs either predicted probabilistically (PFR) or deterministically (DFR).

Validation

A total of 7 validations sets ups were used in this work and were as follows: a lateral pelvis impact (Bouquet, 1998), a shoulder hub impact (Koh, et al., 2005), a chest hub impact (Kroell, et al., 1971; Kroell, et al., 1974), a thoracoabdominal (or oblique) hub impact (Viano, 1989), an abdominal bar impact (Hardy, et al., 2001), a lateral plate impact (Kemper, 2008), and a lateral sled (Cavanaugh, et al., 1990; Cavanaugh, et al., 1993) (Figure 1). These cases were chosen as they give a wide range of impact severities, loading directions and loading areas of the body. These cases were also used in validation of v4.2 of the GHBMC M50-O model (Vavalle, et al., 2015; Vavalle, et al., 2013b).

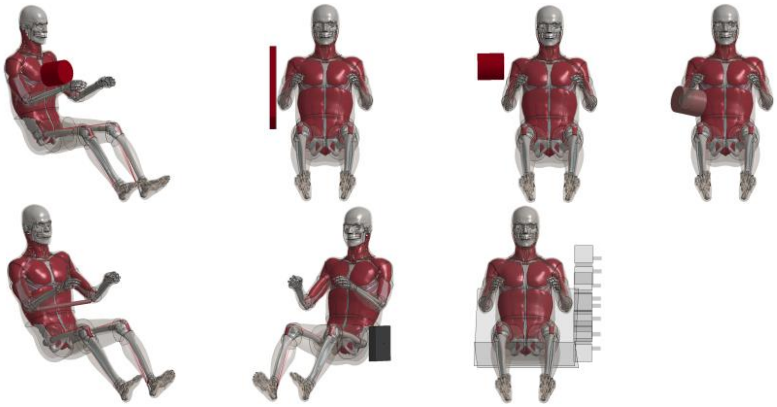

Figure 1: The M50-O model in the various setups that were used throughout the study.

Pelvic Plate. The pelvic plate impact used a 16 kg block impactor that struck the pelvis laterally at 10 m/sec (Bouquet, 1998). The average age of the 4 PMHS considered was 70.3 years.

Lateral Plate. A lateral plate impact was performed using a flat plate impactor with a 23.4 kg mass that struck the shoulder, arm and ribs at 12 m/sec and the arm position corresponds to the data from the 45 degree arm angle experimental tests (Kemper, 2008).

Shoulder Hub. The lateral shoulder impact was performed with a 23.4 kg hub impactor striking the shoulder laterally through the head of the humerus at 4.5 m/sec (Koh, et al., 2005). There were a total of 6 PMHS used in this study with an average age of 54 years.

Chest Hub. The chest hub impact was conducted with a 23.4 kg hub impactor that struck the sternum of the model at the fourth intercostal space as per literature (Kroell, et al., 1971; Kroell, et al., 1974). Data from 7 PMHS with an average age of 58 was used in the comparison.

Thoracoabdominal (Oblique) Hub. A 23.4 kg hub impactor was used to strike the model at 6.7 m/sec 60 degrees from anterior and 7.5 cm below the xiphoid process (Viano, 1989). Data from 6 PMHS with an average age of 55.2 years was considered.

Abdominal Bar. The abdominal bar impact was performed with a 48 kg bar that was rigid that struck the navel at approximately L3 at 6.0 m/sec (Hardy, et al., 2001). There were 3 PMHS with an average age of 88 examined for this impact.

Lateral Sled. A Heidelberg-type sled was used for the lateral sled test and the subject impacted beams that were located at the shoulder, thorax, abdomen, pelvis and knee (Cavanaugh, et al., 1990; Cavanaugh, et al., 1993). The model was initially gravity settled into the seat over a period of 100 msec prior to the application of a lateral 6.7 m/sec velocity. Experimental data for the lateral sled consists of 3 PMHS with an average age of 65 years.

Data Outputs

The ribcage in the M50-O model is meshed with solid and shell elements consisting of hexahedral and quadrilateral elements. Of these elements, cancellous bone is represented by the solid elements while shell elements are representative of cortical bone. Cortical thicknesses was assigned to the rib cage through the use of an element shell thickness card within LS-Dyna. The thicknesses used were derived from mircro-CT (Choi, et al., 2009) and enables spatial specificity in cortical bone thickness. The cortical and cancellous portions of the rib are modeled with a piecewise linear plasticity material model with differing failure strains; the cortical rib material model has a failure strain of 0.018 and the cancellous rib material model has a failure strain of 0.13. The rib failure strains that are used were determined by computational optimization work (Li, et al., 2010b) that used baseline values from literature (Kemper, et al., 2005; Kemper, et al., 2007; Kent, et al., 2005) and then varied young's modulus, tangent modulus, yield stress and failure plastic strains to determine effects on failure location, forces and displacements.

The methods for data extraction and processing for deterministically failed regions (DFRs) are detailed in literature (Guleyupoglu, et al., 2017b) but are briefly summarized here. A total of 68 sections were created with an even distribution on left and right sides. The algorithm extracts rib effective plastic strain data and determines through element connectivity if it qualifies as a DFR. Qualification as a DFR is dependent on there being 4 connected elements in any orientation (Li, et al., 2010a; Vavalle, et al., 2013b). The algorithm and visualization framework was updated to process and display results from a probabilistic framework that can be found in literature (Forman, et al., 2012). To be considered a probabilistic failed region (PFR), a threshold of 90% and a default age of 35 years were used. The chosen threshold facilitates comparison with DFRs in which failures are explicit. The PFR method is dependent on maximum principal strains in the model and is used to calculate the probability of failure in the ribcage of the model. As PFRs are determined regionally (or section by section), the DFR data was also examined section by section for ease of comparison.

Simulations

Simulations were run on a Linux Red Hat 6 high performance computing system (the Distributed Environment for Academic Computing cluster at Wake Forest University) on 48 cores using LS-DYNA v.7.1.2, rev. 95028 (LSTC, Livermore CA).

RESULTS

Overall, both PFR and DFR methods predicted above the average amount of fractures observed experimentally (Figure 2). In the pelvic plate impact, there are no fractures reported and 0 DFRs and PFRs as well. For the lateral plate case, both the DFR (23 failures) and PFR (22 failures) methods were at the experimental values. In the shoulder hub case, both the DFR and PFR methods predicted failures when there were none experimentally. Failures in the chest hub impact for the DFR and PFR methods were lower than the experimental average however was within the range of fractures that occurred (1 DFR and 3 PFRs). In the oblique hub case the amount of failures predicted was greater than the experimentally observed fractures with 9 DFRs and 13 PFRs. DFRs in the abdominal bar case was within the range of fractures seen experimentally (10 DFRs) but the PFR method over predicted (16 PFRs). Finally in the lateral sled case, there is better agreement across all three cases although both DFRs and PFRs predicted above the average.

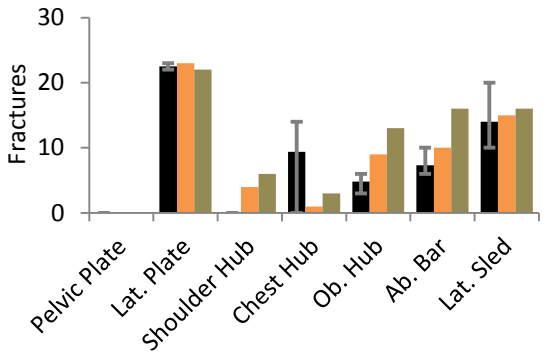

Figure 2: The average amount of fractures in PMHS studies (black) plotted against the amount of DFRs (orange) and PFRs (gold) predicted at the end of the most severe portion of the event. Error bars represent the range of fractures observed experimentally.

The two different methods also had different timings for failure initiation and force profiles with the lateral plate case presented in Figure 3. In the lateral plate impact, failure initiation was offset by 2.5 msec (6 msec PFR and 8.5 msec DFR). However, for the rest of the simulation, both methods tracked closely up until the event ended and the M50-O was rebounding. The DFR method also tended to have failures occur before the PFR method during the impact period. The force profiles experienced by the two models were relatively the same with differences occurring between 11 and 17.5 msec. The higher forces is due to the fact that between this time there have been a significant amount of failures that occurred in the deterministic method that allowed for a force let-off to occur.

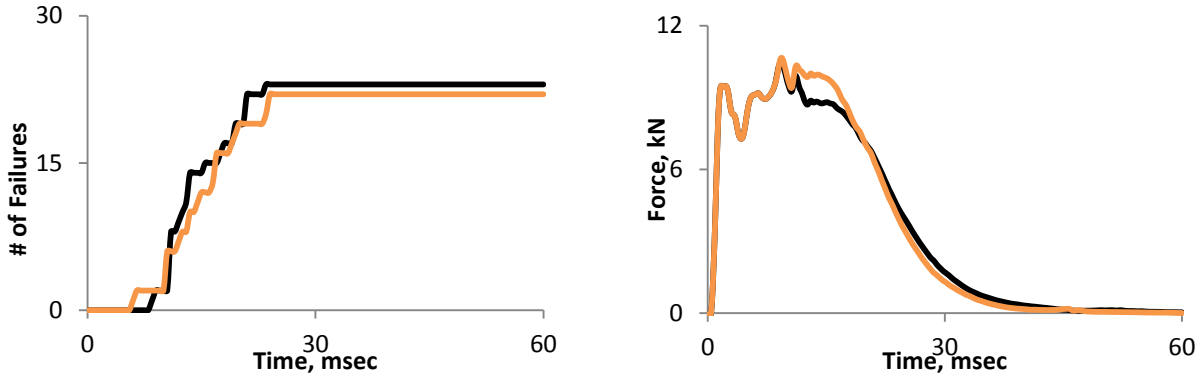

Figure 3: Fracture timing for the lateral plate impact on left and force vs. time profile on right with deterministic in black and probabilistic in orange.

DISCUSSION

In this study, two methods of predicting rib failure in a computational human body model were compared against experimentally determined fractures published in literature. Although ATDs and PMHS are effective tools in evaluating injury, computational human body models allow for effective relatively inexpensive (vs. testing) and repeatable method for determining both correlative and localized injury. Previous studies have evaluated the M50-O rib model against real world data in varying levels of detail however, had demonstrated relatively good performance against fracture data when visually inspected. Of these studies, the most recent one quantified the ribs and locations of fracture and compared it against the fracture data (Davis, et al., 2016). Examining the fractures in this way allows for determination of how well models are performing spatially but also allows for examining a greater range of subjects rather than just the average.

In Table 1 a summary of experimental failures by subject with detail from each study compared against the predictions of the deterministic and probabilistic methods is shown. In the lateral plate case where no fracture was reported, the deterministic and probabilistic methods predicted failure in rib 11. In the study by Forman et al, rib 11 was not evaluated for its prediction capability and may be intrinsically more sensitive (Forman, et al., 2012). In the lateral plate impact, both subjects had 9 posterior fractures and 12 anterior and lateral fractures with 1 or 2 on the non-impacted side of the body. The deterministic method had 6 posterior failures and 12 failures on anterior and lateral aspects for the impacted side while non-impacted had 5. The probabilistic method predicted 3 posterior failures and 13 anterior lateral failures with 11 non-impacted side failures. The impacted side in this case matched anterior/lateral failures closely while posterior failures were lower. In the chest hub case the average fractures was 9.4 however, the actual amounts ranged from 0-14 fractures. Both the deterministic and probabilistic were within this range of predictions. In the abdominal bar case, the PMHS presented fractures bilaterally on ribs 6 through 10. The DFR and PFR predictions both had bilateral failures for ribs 6-9 and 11. The PFR method also predicted bilateral failures for rib 10, which was present in one of the three subjects. While the two methods may not match the average fractures that were

present in each study, they demonstrate capability to predict similar failure patterns but could use further refinement.

The PFR method does not predict individual FRs within a section rather an overall risk of injury within that section. However, it is advantageous in that predictions for this method for varying ages can be done in post-processing rather than having to rerun the model (Forman, et al., 2012). A default age of 35 was used in this study however the predictions can be easily adjusted for by age. The DFR method would require changes to ultimate strain and potentially to the entire material model to achieve the same age sensitivity as the PFR method. In theory, the PFR method can more readily adjust for age and shows promise in predicting rib failures.

There were a number of assumptions and limitations made in the execution of this study. The rib model that was implemented in the M50-O model is a hybrid of different ages. The ribcage shape is representative of a 26 year old male while the material properties are closer to that of an older male as they were derived from cadaveric studies (Schoell, et al., 2015). Micro-CT derived thicknesses for cortical bone can influence FR predictions because the varying thickness can cause some areas to fail earlier than others. While studies that compared experimental fractures to those predicted from the GHBMC model, the goal of this study was to quantify the differences between what the automated tool predicted and what was determined experimentally. Also, in this study, only a single element per section was used to determine probabilistic failure and strain hotspots (multiple connected elements) may help refine PFR predictions. Future work will include more cases in which fractures have been determined experimentally and will use a sensitivity analysis to further refine the predictions from these tools.

Table 1: Rib failure predictions of the deterministic and probabilistic methods against individual experimental injury reports from literature.

	Experiment	**Deterministic**	**Probabilistic**
Pelvic Plate	No Fracture	No Fracture	No Fracture
Lateral Plate	9 Posterior, 12 Anterior and Lateral. 1 Non-impacted side	Bilateral rib 1. Right ribs 2, 3, 4, 5, 6, 7, and 8. Left rib 9, 10, 11.	Bilateral rib 1, 8, 9, 11. Right rib 2, 5, 6, and 7. Left rib 10.
	9 Posterior, 12 Anterior and Lateral, 2 non-impacted side.		
Shoulder Hub	No Fracture	Left rib 1. Right rib 2, 6, 11.	Bilateral rib 11. Right rib 7. Left rib 1 and 9.
Chest Hub	0-14 Rib fractures	Left rib 11.	Bilateral rib 11. Left rib 9.
Oblique Hub	Ribs 7, 8, 9	Right ribs 6, 7, 8, 9, 10, and 11	Bilateral ribs 6, 7, 10, and 11. Right ribs 8 and 9
	Ribs 6, 7, 8, 9, 10		
	Ribs 7, 8		
	No Fracture		
Abdominal Bar	Bilateral fracture ribs 7, 8 ,9	Bilateral ribs 6, 7, 8, 9, and11.	Bilateral ribs 6, 7, 8, 9, 10 and 11.
	Bilateral fracture ribs 6, 7, 8, 9, 10		
	Bilateral ribs 7 and 8. Left ribs 6 and 7		
Lateral Sled	Flail chest. 5 flail ribs	Right ribs 1, 9, 11. Left ribs 2, 4, 5, 6, 7, 8.	Bilateral rib 1, 8. Left ribs 2, 5 and 6 7. Right rib 9, 10, 11
	Flail chest. 5 flail ribs		
	Bilateral flail chest		

CONCLUSIONS

Both methods predicted a greater number of failures for most cases at the end of the simulation. When the time point at which data was analyzed was adjusted for by the time which the impact imparted its energy into the model, better agreement was found between experimental data and both the DFR and PFR methods. Failure timing demonstrates the differences between the two methods with probabilistic failure initiating before deterministic. When the failures were compared on a fracture by fracture basis from experimental results, the two methods demonstrated capability to accurately predict where these fractures were occurring. The probabilistic method is advantageous due to the fact that it is a post-processing method and can readily account for age.

ACKNOWLEDGEMENTS

Work was supported by Wake Forest University School of Medicine, the Global Human Body Models Consortium, LLC and NHSTA under GHBMC Project No.: WFU-005. All simulations were run on the DEAC cluster at Wake Forest University, with support provided by Drs. David Chin and Timothy Miller. F. Scott Gayzik is a member of Elemance, LLC., which distributes academic and commercial licenses for the use of GHBMC-owned computational human body models.

REFERENCES

1. Barker JB, Cronin DS, Nightingale RW. Lower Cervical Spine Motion Segment Computational Model Validation: Kinematic and Kinetic Response for Quasi-Static and Dynamic Loading. *Journal of Biomechanical Engineering.* 2017;139(6):061009-061009-061011.

2. Bouquet R, Ramet, M., Bermond, F., Caire, Y., Talantikite, Y., Robin, S., Voiglio, E. Pelvis human response to lateral impact. Paper presented at: 16th International Technical Conference on the Enhanced Safetfy of Vehicles1998; Windsor, ON, Canada.

3. Cavanaugh JM, Walilko TJ, Malhotra A, Zhu Y, King AI. Biomechanical Response and Injury Tolerance of the Pelvis in Twelve Sled Side Impacts. *SAE.* October 1990 1990:16.

4. Cavanaugh JM, Zhu Y, Huang Y, King AI. Injury and Response of the Thorax in Side Impact Cadaveric Tests. *SAE.* 1993:23.

5. Choi HY, Han J, Park Y, Yoon KH. Digital Elderly Human Body Modeling: SAE International; 2009.

6. Davis M, Koya B, Schap J, Gayzik FS. Development and full body validation of a 5th percentile female finite element model. *Stapp Car Crash Journal.* 2016;60:509-544.

7. Decker W, Koya B, Davis M, Gayzik FS. Modular use of human body models of varying lvels of complexity: validation of head kinematics. *Traffic Inj Prev.* 2017.

8. DeWit JA, Cronin DS. Cervical spine segment finite element model for traumatic injury prediction. *Journal of the mechanical behavior of biomedical materials.* 2012;10:138-150.

9. Fice JB, Cronin DS, Panzer MB. Cervical spine model to predict capsular ligament response in rear impact. *Annals of biomedical engineering.* 2011;39(8):2152-2162.

10. Forman J, Kent R, Mroz K, Pipkorn B, Bostrom O, Segui-Gomez M. Predicting Rib Fracture Risk With Whole-Body Finite Element Models: Development and Preliminary Evaluation of a Probabilistic Anayltical Framework. *Traffic Inj Prev.* 2012;56:109-124.
11. Gayzik FS, Moreno DM, Geer CP, Wuertzer SD, Martin RS, Stitzel JD. Development of a Full Body CAD Dataset for Computational Modeling: A Multi-Modality Approach. *Annals of Biomedical Engineering.* 2011;39(10):2568-2583.
12. GHBMC. User Manual: M50 Occupant Version 4.3 for LS-DYNA2014.
13. Guleyupoglu B, Barnard R, Gayzik FS. Automating Regional Rib Fracture Evaluation in the GHBMC Detailed Average Seated Male Occupant Model. *SAE World Congress 2017*. Detroit, MI2017b:1-8.
14. Hardy WN, Schneider LW, Rouhana SW. Abdominal impact response to rigid-bar, seatbelt, and airbag loading. *Stapp car crash journal.* 2001;45:1-32.
15. Hayes AR, Vavalle NA, Moreno DP, Stitzel JD, Gayzik FS. Validation of simulated chestband data in frontal and lateral loading using a human body finite element model. *Traffic Inj Prev.* 2014;15(2):181-186.
16. Kemper AR, McNally C, Kennedy EA, et al. Material properties of human rib cortical bone from dynamic tension coupon testing. *Stapp Car Crash J.* Nov 2005;49:199-230.
17. Kemper AR, McNally C, Pullins CA, Freeman LJ, Duma SM, Rouhana SM. The biomechanics of human ribs: material and structural properties from dynamic tension and bending tests. *Stapp Car Crash J.* Oct 2007;51:235-273.
18. Kemper AR, McNally, C., Duma, S.M. Dynamic tensile material properties of human pelvic cortical bone. *International IS Biomedical Sciences Instrumentation Symposium.* 2008.
19. Kent R, Sang-Hyun L, Darvish K, Wang S, al e. Structural and material changes in the aging thorax and their role in crash protection for older occupants. *Stapp Car Crash Journal.* 2005;49:231-249.
20. Kim YH, Kim JE, Eberhardt AW. A new cortical thickness mapping method with application to an in vivo finite element model. *Comput Methods Biomech Biomed Engin.* Oct 31 2012;17(9):997-1001.
21. Koh SW, Cavanaugh JM, Mason MJ, et al. Shoulder injury and response due to lateral glenohumeral joint impact: an analysis of combined data. *Stapp Car Crash J.* Nov 2005;49:291-322.
22. Kroell C, Schneider D, Nahum A. Impact Tolerance and Response of the Human Thorax. *Stapp Car Crash J.* 1971;15.
23. Kroell CK, Schneider DC, Nahum AM. Impact tolerance and response of the human thorax II. *SAE Technical Paper.* 1974;741187.
24. Li Z, Kindig MW, Kerrigan JR, et al. Rib Fractures Under Anterior-Posterior Dynamic Loads: Experimental and Finite-Element Study. *Journal of Biomechanics.* 2010a;43:228.234.
25. Li Z, Kindig MW, Subit D, Kent RW. Influence of mesh density, cortical thickness and material properties on human rib fracture prediction. *Medical engineering & physics.* 2010b;32(9):998-1008.
26. Mao H, Zhang L, Jiang B, et al. Development of a Finite Element Human Head Model Partially Validated With Thirty Five Experimental Cases. *Journal of biomechanical engineering.* 2013;135(11):111002.

27. Mattucci SF, Moulton JA, Chandrashekar N, Cronin DS. Strain rate dependent properties of human craniovertebral ligaments. *Journal of the mechanical behavior of biomedical materials.* 2013;23:71-79.
28. Mattucci SF, Moulton JA, Chandrashekar N, Cronin DS. Strain rate dependent properties of younger human cervical spine ligaments. *Journal of the mechanical behavior of biomedical materials.* 2012;10:216-226.
29. Park G, Kim T, Crandall JR, Arregui-Dalmases C, Luzon-Narro J. Comparison of Kinematics of GHBMC to PMHS on the Side Impact Condition. *International Research Council on Biomechanics of Injury*. Gothenburg, Sweden2013.
30. Pattimore D, Thomas P, Dave S. Torso injury patterns and mechanisms in car crashes: an additional diagnostic tool. *Injury.* 1992;23(2):123-126.
31. Poulard D, Kent R, Kindig M, Li Z, Subit D. Thoracic response targets for a computational model: A hierarchical approach to asses the biofidelity of a 50th-percentile occupant male finite element model. *J Mech Behav Biomed Mater.* 2015.
32. Schoell S, Weaver A, Jillian U, Jones D, Stitzel JD. Development and Validation of an Older Occupant Finite Element Model of a Mid-Sized Male for Investigation of Age-related Injury Risk. *Stapp Car Crash Journal.* 2015;59:1-25.
33. Shin J, Untaroiu C. Biomechanical and Injury Response of Human Foot and Ankle under Complex Loading. *J Biomech Eng.* Jul 1 2013;135(10).
34. Soni A, Beillas P. Modelling hollow organs for impact conditions: a simplified case study. *Comput Methods Biomech Biomed Engin.* Oct 24 2013;[Epub ahead of print].
35. Takhounts EG, Craig MJ, Moorhouse K, McFadden J, Hasija V. Development of Brain Injury Criteria (BrIC). *Stapp car crash journal.* 2013;57:243-266.
36. Untaroiu CD, Yue N, Shin J. A finite element model of the lower limb for simulating automotive impacts. *Ann Biomed Eng.* Mar 2013;41(3):513-526.
37. Vavalle N, Davis M, Stitzel JD, Gayzik FS. Quantitative validation of ahuman body finite element model using rigid body impacts. *annals of biomedical engineering.* 2015;43(9):2163-2174.
38. Vavalle NA, Davis ML, Stitzel JD, Gayzik FS. Quantitative Validation of a Human Body Finite Element Model Using Rigid Body Impacts. *Annals of Biomedical Engineering.* 2014:1-12.
39. Vavalle NA, Jelen BC, Moreno DP, Stitzel JD, Gayzik FS. An evaluation of objective rating methods for full-body finite element model comparison to PMHS tests. *Traffic Inj Prev.* 2013a;14 Suppl:S87-94.
40. Vavalle NA, Moreno DP, Rhyne AC, Stitzel JD, Gayzik FS. Lateral impact validation of a geometrically accurate full body finite element model for blunt injury prediction. *Ann Biomed Eng.* Mar 2013b;41(3):497-512.
41. Vavalle NA, Thompson AB, Hayes AR, Moreno DP, Stitzel JD, Gayzik FS. Investigation of the Mass Distribution of a Detailed Seated Male Finite Element Model. *J Appl Biomech.* Dec 17 2013c;[Epub ahead of print].
42. Viano DC. Biomechanical Responses and Injuries in Blunt Lateral Impact. *Stapp Car Crash J.* 1989;33.
43. Yanaoka T, Dokko Y. A Parametric Study of Age-Related Factors Affecting Intracranial Responses under Impact Loading Using a Human Head/Brain FE Model. *International Research Council on Biomechanics Injury (IRCOBI)*. Gothenburg, Sweeden2013.

44. Yue N, Shin J, Untaroiu C. Development and validation of an occupant lower limb finite element model. *SAE Technical Paper*2011.
45. Yue N, Untaroiu CD. A numerical investigation on the variation in hip injury tolerance with occupant posture during frontal collisions. *Traffic Injury Prevention.* 2014;15(5):513-522.